

# Improved Operational Trans-Conductance Amplifier for Bio-potential Signals

Lipika Gupta<sup>1</sup>, Amod Kumar<sup>2</sup>

<sup>1</sup>Chitkara University School of Engineering and Technology, Chitkara University, Himachal Pradesh, India

<sup>2</sup>National Institute of Technical Teachers Training and Research, Chandigarh.

## Article Info

Volume 83

Page Number: 17 – 26

Publication Issue:

March -April 2019

## Article History

Article Received: 24 January 2019

Revised: 12 February 2019

Accepted: 15 March 2019

Publication: 30 April 2019

## Abstract

Bio-potential signals are acquired non-invasively using surface electrodes. These electrodes are followed by the pre-amplifiers to provide amplification to these low frequency and low amplitude signals for further processing. This work focuses on the design of the first-stage Operational Trans-Conductance Amplifier (OTA) used as pre-amplifier. Capacitive coupled current mirror OTA is designed to obtain the optimized values of bandwidth, power, noise and area. The modification in feedback circuit elements i.e. pseudo-resistors' structures, feedback capacitors and coupling capacitors were considered to remove the limitations of non-linearity and large area. The two-series-connected pMOS and back-to-back source connected pMOS structure based pseudo-resistors enhanced the performance of the OTA, whereas, the T-capacitor network based feedback significantly reduced the area of the OTA.

**Keywords:** Operational Trans-Conductance Amplifier,  $g_m/I_D$  method, Current mirror, Pseudo-resistor, T-Capacitor network.

## I. Introduction

Operational Trans-conductance Amplifier (OTA) is widely used as first stage of front-end amplifiers (FEAs) particularly for bio-potential measurements [1], [2]. Bio-potential signals such as Electrocardiography (ECG), Electroencephalography (EEG), Electromyography (EMG), Electrooculography (EOG) etc. are acquired non-invasively using the surface electrodes. These body signals being very low frequency and low amplitude signals require amplification and signal conditioning. Therefore, amplification of signals at first-stage plays a vital role to regulate the overall performance of the Bio-potential amplifier. The OTA used at this stage can devour high power, noise and area in a multi-electrode bio-potential measurement system [3],

[4]. Therefore, it is important to meticulously design OTA having the specific parameters viz. high input impedance (100 M $\Omega$ -10 T $\Omega$ ), suitable gain (Open loop gain  $\geq$  40 dB), limited bandwidth (< 10 kHz) to improve the signal-to-noise ratio, low input referred noise (< 5  $\mu$ V/ $\sqrt$ Hz), Common mode rejection ratio (CMRR) (>60 dB) and Power supply rejection ratio (PSRR) (>40 dB) while ennobling the bio-signal [3], [5]–[8].

Numerous OTA topologies and architectures have been highlighted in the literature of bio-potential amplifiers. Conventional two-stage Miller OTA [9]–[13] was used for multiple neural signal modalities, such as local field potentials (LFP), electrocorticograms (ECoG) and electroencephalograms (EEG). Also, conventional Telescopic amplifier topology offers low power dissipation, low-noise and medium gain [14].

Several researchers have used this topology, Shahrokhi et al. [15] used telescopic OTA with current mode, claiming that high dynamic range is not an important parameter for the first stage of amplifier. The first stage of telescopic OTA was shared among different channels to design an energy efficient solution for multichannel neural amplifiers [16]. Similarly, use of conventional folded cascode topology was elaborated by many researchers [17]–[20].

Current-mirror-OTA [5] was subjugated by many researchers; the neural amplifier introduced by Harrison and Charles [2003] is one of the most significant contributions to extract EEG. In this topology the gain of the amplifier depends on the value of feedback and coupling capacitors. While the size of the capacitors increases the area of the amplifier, active feedback topology was used to diminish the size of the amplifier by eradicating input capacitors and RC feedback network [21]. However, the noise and power consumption of the circuit was increased. Later, current reuse technique for differential amplifier stage and T-network capacitors in the feedback improved power efficiency [22]. Area reduction achieved by replacing feedback capacitor by capacitive T-Network along with tunable pseudo-resistor was initially explained by Ng and Xu [23], however, this design increased input-noise. Recently, Benko et al. [24] exploited the non-linear characteristics of Pseudo-resistors which eliminated the need of high capacitive elements in feedback circuit of current-mirror topology. This helped to reduce area and offset DC level input while preserving the low cut-off frequency.

The focus of this work is to design reduced area OTA using current mirror topology in closed loop configuration. From the literature survey, it is clear that size of coupling and feedback capacitors significantly increases the area of the amplifier. Smaller capacitances decrease the gain and CMRR of the circuit [18]; sharing the input capacitors among the multiple channels leads to cross-talk and deteriorates the acquired bio-potential signal.

Conversely, T-capacitor network can be used to effectively reduce the size of the capacitors without significant decrease in gain.

In this paper, a T-capacitor based OTA is designed using current-mirror topology on 0.18 $\mu$ m technology node BSIM3V3 MOS Transistor Model from Cadence Virtuoso. Section 2 discusses design and implementation of T-capacitor based OTA, Section 3 explains the results obtained and presents the comparison of designed current mirror OTAs. Finally, section 4 concludes the paper.

## II. DESIGN AND IMPLEMENTATION OF T-CAPACITOR BASED OTA

### Basics Current mirror OTA:

Fig. 1(a) refers to Current mirror topology, where input transistors  $M_1$  and  $M_2$  are pMOS devices. MOSFET pairs ( $M_3, M_5$ ), ( $M_4, M_6$ ) and ( $M_7, M_8$ ) are three current mirrors pairs used to mirror the input differential voltage to current output.  $M_9$  and  $M_{10}$  are used to bias the input devices.  $M_{cascp}$  and  $M_{casen}$  are the cascoding devices for gain boosting [5], [8].

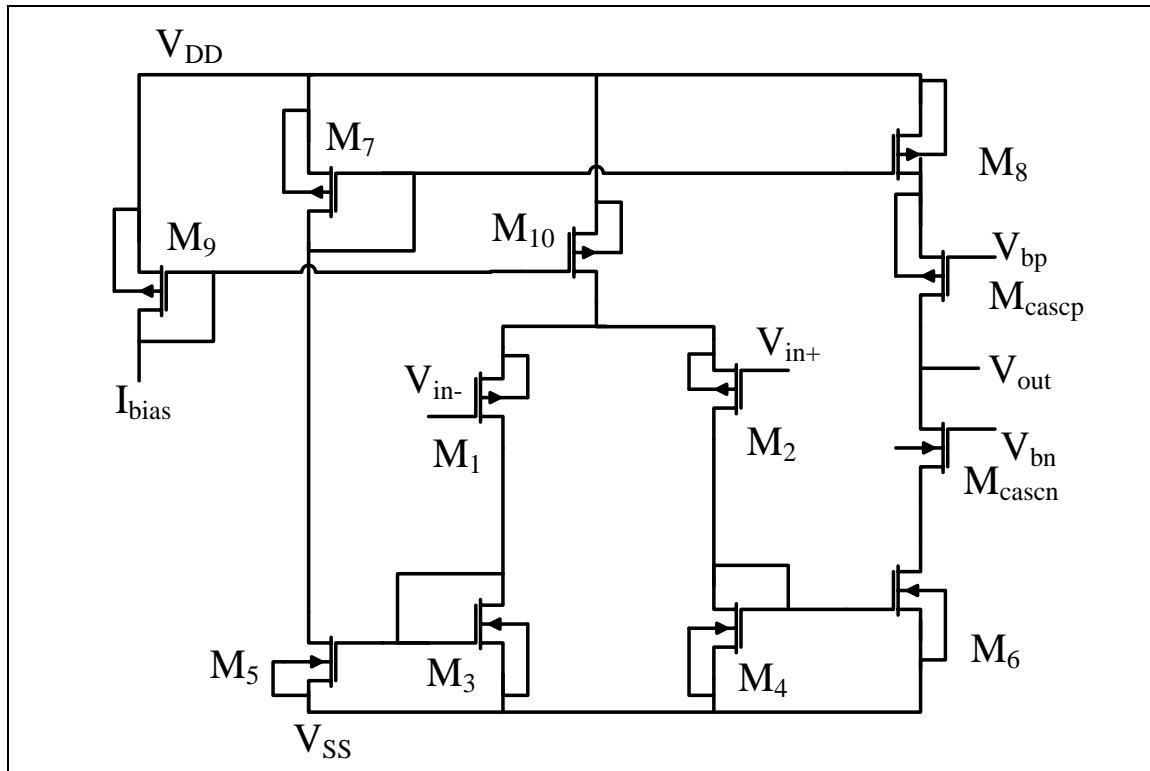
The OTA with capacitive feedback architecture is shown in Fig. 1(b), the mid-band gain and bandwidth of the amplifier was calculated using the values the coupling ( $C_1$ ), feedback ( $C_2$ ) and load capacitors ( $C_L$ ). The output current of the OTA is proportional to the differential voltage applied to its inputs  $v_{in+}$  and  $v_{in-}$  given by equation (1).

$$i_{out} = g_m(v_{in+} - v_{in-}) \quad (1)$$

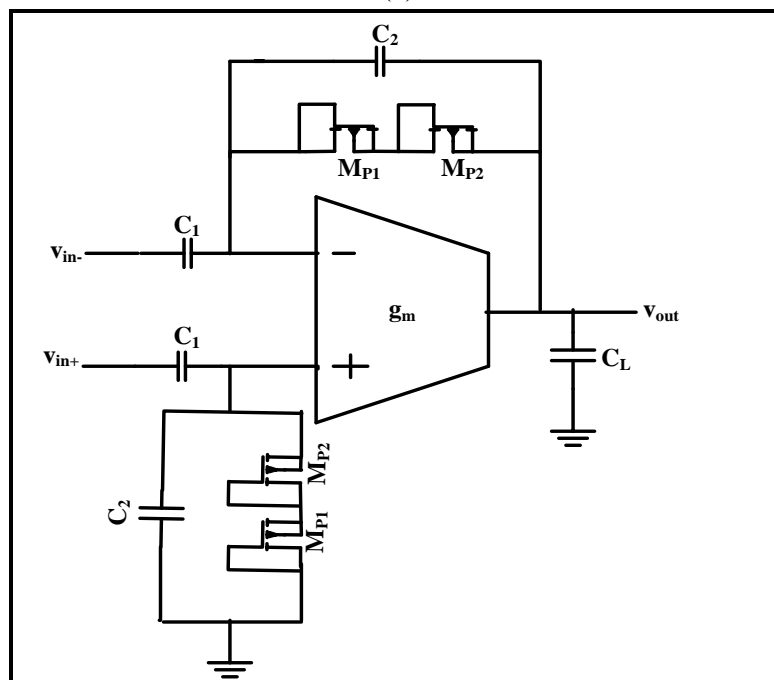
where  $g_m$  is the trans-conductance of the amplifier. The mid-band gain of OTA is given by  $A_m = C_1/C_2$ . Bio-potential inputs acquired from electrode-tissue interface are capacitively coupled with  $C_1$ . This coupling is responsible for removal of the DC offset generated due to electrode-tissue interface. The lower cut-off frequency of the amplifier is depended on the value of pseudo-resistors formed by diode connected  $M_{P1}$  and  $M_{P2}$  ( $R \geq 10^{12} \Omega$ ).  $C_L$  is the load capacitor and determines the upper cut-off frequency of OTA. It also acts as short-circuit

impedance for high frequency noise, thereby passing only the useful low frequency bio-signals. The differential gain ( $A_d$ ) is given by eq. (2), where  $s$  is the Laplace Operator.

$$A_d = \frac{v_{out}}{v_{in+} - v_{in-}} = \frac{C_1}{C_2} \cdot \frac{1 - s \frac{C_2}{g_m}}{\left(\frac{1}{sRC_2} + 1\right) \left(s \frac{C_L C_1}{g_m C_2} + 1\right)} \quad (2)$$



(a)



(b)

Fig. 1 (a) Current mirror topology for OTA (b) Closed Loop OTA with capacitive feedback [5]

### OTA with feedback as T-Capacitive Network:

The single feedback capacitor  $C_2$  in Fig. 1(b) significantly increases the area of the OTA. Whereas reducing the value of  $C_2$  reduces the gain of the amplifier. Also, the area occupied by the coupling capacitor  $C_1$  is large due to its value which is useful to reject the DC-offset due to electrode-scalp interface. In order to reduce the effective area of the amplifier,  $C_1$  and  $C_2$  can be replaced by a T-capacitive network.

Consider Fig. 2,  $C_1$  of the OTA (Fig. 1(b)) is replaced by  $C_1 = M \times C_u$ , where  $M$  is the mid-band gain factor ( $C_1/C_2$ ) and  $C_u$  is a unit capacitor.  $C_1$  is multiple of the unit capacitor ( $C_u$ ) such that the mid-band gain remains same.

$C_2$  is replaced T-shaped capacitive network comprising of  $C_u$  and  $C_4$  (shunt capacitor). Here, equivalent feedback capacitance ( $C_{fb}$ ) of the T-capacitor network and is given by:

$$C_{fb} = \frac{C_u}{(N+2)} \quad (3)$$

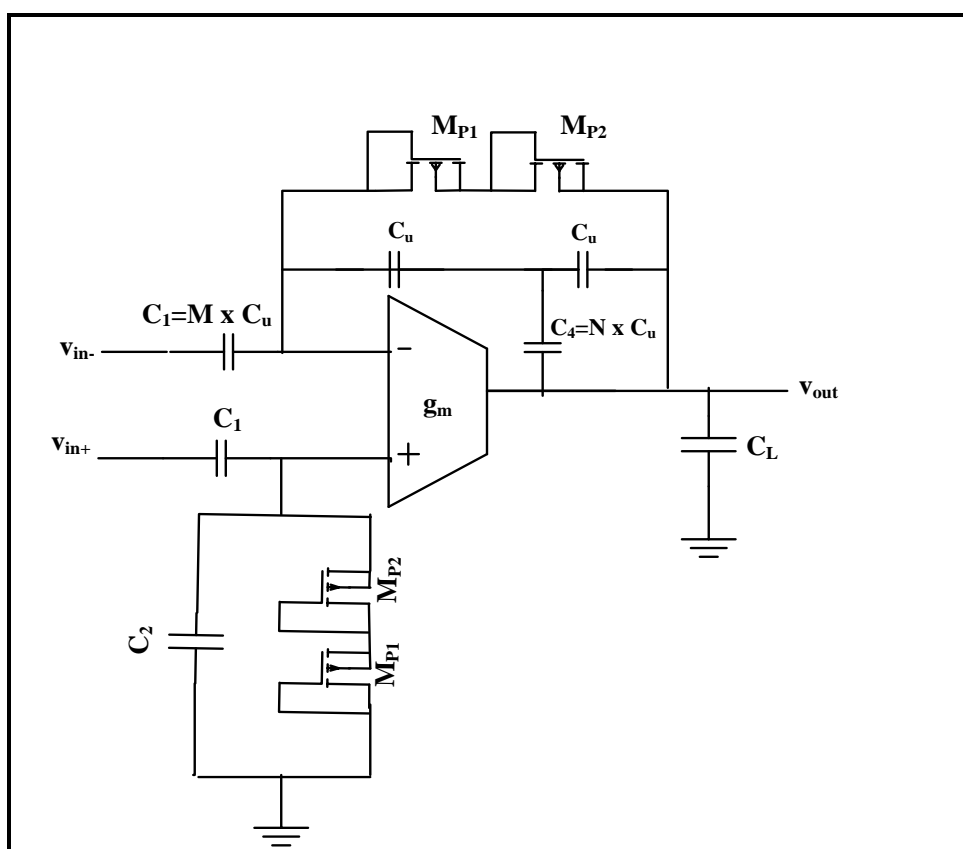


Fig. 2: Current Mirror OTA with T-capacitor feedback network [23]

### III. RESULTS AND DISCUSSIONS

In this work, current-mirror OTA was designed using  $g_m/I_D$  methodology (Fig. 1(a)) [25]. Using the 180nm technology node, the OTA was simulated in Cadence virtuoso using BSIM3V3 MOS Transistor Model. Considering bio-potential signals of very low amplitude and frequency signals such as EEG and EMG, the values of  $C_1$ ,  $C_2$  and  $C_L$ , were set at 20 pF, 200 fF and 50 pF respectively (Fig. 1 (b)) to obtain the gain of 40

dB, the bandwidth was approximated to 30 Hz. Lower bandwidth of the amplifier can be achieved by providing low bias current; therefore, the bias current was kept to be 74 nA and hence low value of trans-conductance ( $g_m$ ) was obtained. Bias current in turns set the drain current through the devices  $M_1$ -  $M_8$  to 37 nA. Henceforth,  $g_m/I_D$  method and mentioned value of drain current helped to find the aspect ratio (W/L) of MOSFETs ( $M_1$  to  $M_{10}$ ) for the desired operating point in moderate or sub-threshold region. The operation

of transistors in moderate and sub-threshold region reduces the overall power consumption of the OTA [26]. The calculated W/L values were further optimized for low power and low noise to

obtain the desired gain as close as possible. Table 1 shows the operating regions and W/L ratios of all the transistors in the circuit [8].

**Table-1: Operating points of current mirror OTA MOSFETs**

Device	W/L(μm)	I <sub>D</sub> (nA)	g <sub>m</sub> /I <sub>D</sub> (S/A)	Operating region
M <sub>1</sub> , M <sub>2</sub>	5.5/0.27	37	27	Sub-threshold
M <sub>3</sub> , M <sub>4</sub> , M <sub>5</sub> , M <sub>6</sub>	0.45/18	37	15	Moderate
M <sub>7</sub> , M <sub>8</sub>	0.84/7.2	37	15	Moderate
M <sub>9</sub> , M <sub>10</sub>	0.4/0.45	74	15	Moderate
M <sub>cascN</sub>	1.23/0.18	37	27	Sub-threshold
M <sub>cascP</sub>	3.3/0.18	37	27	Sub-threshold

The input signal of 20 Hz, 20 μV was applied for the initial testing and then the frequency of the signal varied to test the response of the system. The input is applied at the inverting end of the amplifier (Fig. 1 (b)).

Diode connected MOSFETs are used as Pseudo-resistors in the feedback of closed loop OTA (Fig. 1(b)). These MOSFETs also work in sub-threshold or triode region to offer very large value of equivalent resistance (~ Tera-ohms). These pseudo-resistors, however, behaves non-linearly when exposed to large voltage swing at the output of amplifier [27]. From eq. (2), mid-band gain of the amplifier A<sub>M</sub> is given by C<sub>1</sub>/C<sub>2</sub> and the high-

pass pole (1/RC<sub>2</sub>). This high-pass pole appears to be time-variant due to non-linearity of pseudo-resistor. In this work, two different structures of diode connected MOSFETs were considered. Two series connected pMOS and Back-to-Back source connected pMOS structure [7] shown in Fig. 3. These structures were used to implement pseudo-resistor (MP<sub>1</sub> and MP<sub>2</sub>) (Fig. 1(b)). The aspect ratio of two series connected pMOS was considered  $\left(\frac{W}{L}\right)_{\mu m} = \left(\frac{0.2}{0.18}\right)$  and for Back-to-Back source connected pMOS was kept to be  $\left(\frac{W}{L}\right)_{\mu m} = \left(\frac{0.45}{0.54}\right)$ .

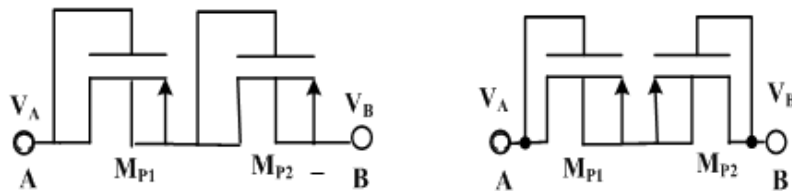


**Fig. 3:** (a) Two-series connected pMOS (b) Back to back source-connected pMOS [7]

T-capacitor network was used to reduce the effective area of Telescopic OTA based neural amplifier [23]. In this work the T-capacitor feedback network was used to replace the feedback and coupling capacitors of current mirror OTA. From Fig. 2, the capacitor C<sub>1</sub> was considered to be

1.5 pF, the value of C<sub>u</sub> is assumed to be 20 fF, such that, N=2/3 which gives C<sub>4</sub>=14 fF and C<sub>fb</sub>=15 fF. These values of C<sub>1</sub>, C<sub>u</sub> and C<sub>4</sub> ensured the mid-band gain of 40 dB and significantly reduced the effective area of the amplifier.

The open-loop gain of T-capacitor based OTA was obtained to be 45.11 dB as compared to 45.

83 dB of current mirror OTA with Two-series connected pMOS as shown in Fig. 4.

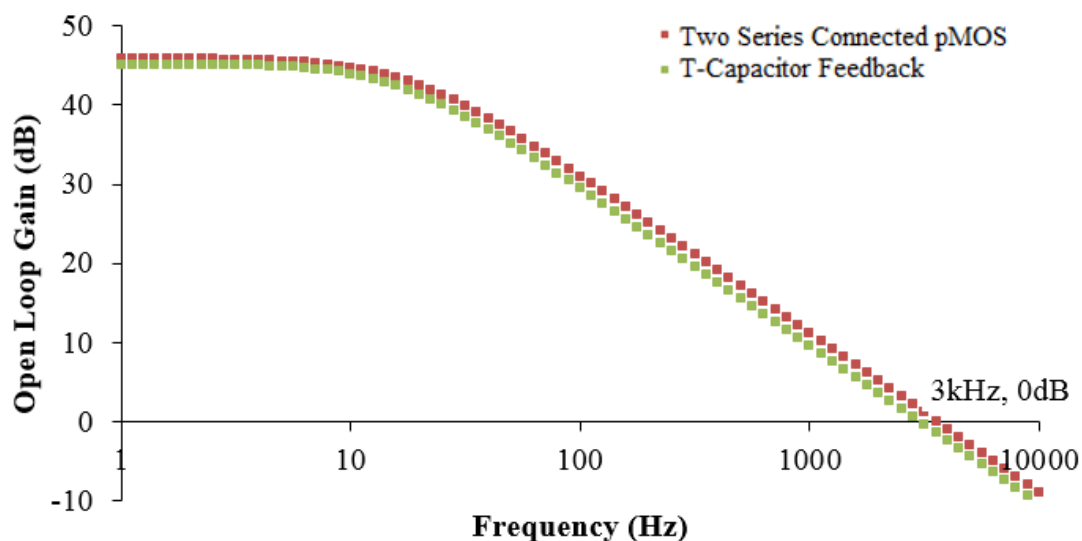


**Fig. 4:** Open-loop gain of Current Mirror OTA

The comparison of the closed loop gain obtained for T-capacitor network based current mirror OTA and closed loop OTA with capacitive feedback is shown in Fig. 5. The results show that the maximum gain is reduced by 1.3 dB. The closed-loop gain for T-capacitor based CCIA is obtained

as 36.17 dB, however, the lower frequency pole shifted to 17 Hz due to decrease in the value of feedback capacitor. The Noise spectrum is compared in Fig. 6 which depicts that the increase in overall input referred noise of T-capacitor based current mirror OTA has increased significantly.

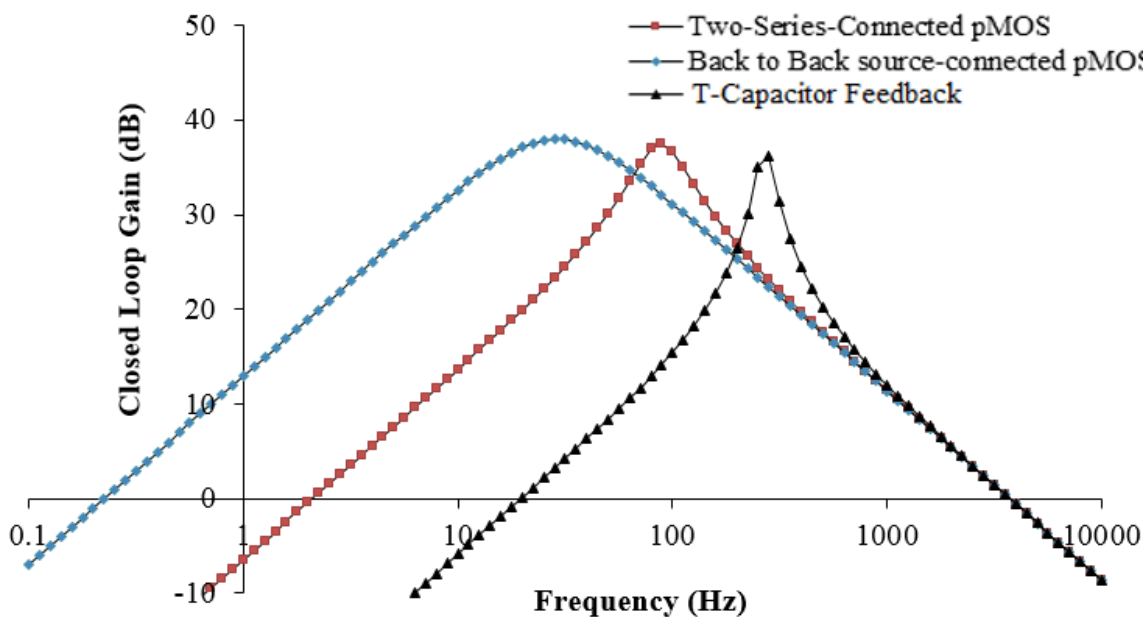


**Fig. 5:** Simulation results of closed-loop gain vs. frequency of Current Mirror OTA

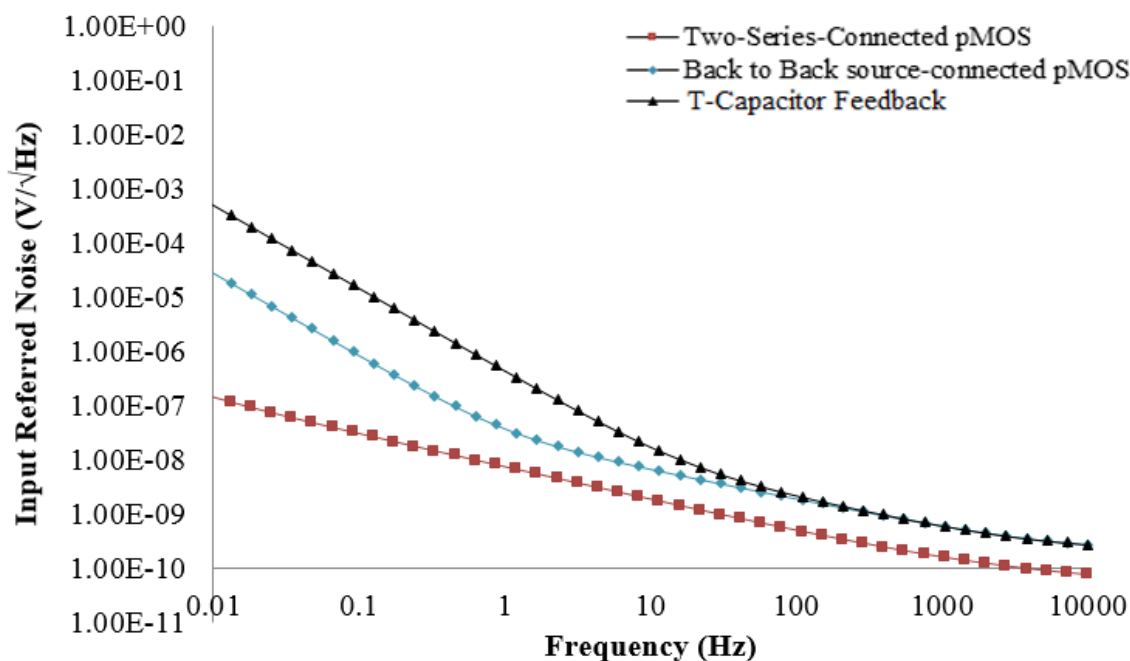


**Fig. 6:** Simulated input-referred voltage noise spectrum of Current Mirror OTA

Table-2 mentions the desired performance metrics of a bio-potential amplifier. The values of all performance metrics for current mirror OTA with capacitive feedback using two-series-connected pMOS, Back-to-Back source connected pMOS and T-Capacitor feedback are also compared in Table 2. The designed OTAs meet the desired specifications and hence suitable for first-stage amplification of bio-potential signals. The capacitors  $C_1=20$  pF and  $C_2=200$  fF are used in two-series-connected pMOS and Back-to-Back source connected pMOS. For T-Capacitor feedback network, the value of the coupling capacitor is reduced from 20 pF to 1.5 pF, whereas the value of feedback capacitor is reduced from

200 fF to 20 fF. Hence, 92.5% of area has been saved by reducing the value of coupling capacitance and 90% area is saved due to reduction in feedback capacitor value. The reduction in area in T-capacitor feedback network is compromised with the increase in noise, higher value of lower cut-off frequency. However, the calculated values of all performance metrics viz. Noise Efficiency factor (NEF) of 5.7 ( $< 6$ ), Open loop gain of 45.11 dB, bandwidth of 17 Hz-3 kHz, CMRR, PSRR are obtained within the desired range. Table-2 also gives the comparison of the designed current mirror OTAs with the existing closed-loop capacitive feedback based bio-potential amplifiers.

**Table-2: Performance metrics of Current Mirror OTA with Capacitive Feedback**

Performance Metric	Technology ( $\mu\text{m}$ )	Open-Loop Gain (dB)	Bandwidth (Hz)	Noise ( $\mu\text{V}/\sqrt{\text{Hz}}$ )	Power consumption ( $\mu\text{W}$ )	CMRR (dB)	PSRR (dB)	NEF
Desired Specifications	0.18	$\geq 40$	$< 10\text{k}$	$< 5$	$< 100$	$> 60$	$> 40$	$< 6$

Two-series connected pMOS	0.18	45.83	1.4-3k	5.28	0.833	$\geq 93$	$\geq 80$	1.629
Back to Back source-connected pMOS	0.18	37.94	0.25-3k	24.74	1.013	$\geq 57$	$\geq 40$	3.24
T-Capacitor feedback	0.18	45.11	17-3k	43.6	0.374	$\geq 54$	$\geq 40$	5.7
[5]	1.5	39.5	0.025-7.2k	2.2	0.9	$> 83$	$> 85$	4.8
[22]	0.18	45.2-59.7	1-10.02k	3.28	4.1	76	80	4.37
[23]	0.35	37.2 – 38.1	1-10k	10.6 -19.1	6	N/A	N/A	5.78-11
[28]	0.18	39.4	10-7.2k	3.5	7.92	70.1	63.8	3.35
[21]	0.18	50	105-9.2k	5.6	8.6	$> 45$	$> 45$	4.6
[29]	0.13	40.5	0.4-8.5k	3.2	12.5	N/A	60	4.5

#### IV. CONCLUSION

In this paper, a capacitively coupled Current Mirror OTA in closed loop configuration designed and optimized to enable the amplification of bio-potential signals at the first stage. Limitations posed due to large area occupied by coupling and feedback capacitors and non-linearity of pseudo-resistors are highlighted. An attempt has been made to reduce these limitations by using two different pseudo-resistor structures and T-capacitor network in feedback of current mirror OTA. OTAs designed using capacitive feedback and Back to Back source connected pMOS and Two-series connected pMOS structures have lower cut-off frequency of 0.25 Hz and 1.4 Hz. Also, T-capacitor network based current mirror OTA reduced the area by 90% by using lower value coupling and feedback capacitors. The OTA designs meet most of the desired performance metrics for low amplitude and low-frequency bio-potential signal amplification. The proposed designs can be further optimized to obtain lower noise and power.

#### REFERENCES

- [1] B. Gosselin and M. Sawan, "An ultra low-power CMOS automatic action potential detector," *IEEE Trans. Neural Syst. Rehabil. Eng.*, vol. 17, no. 4, pp. 346–353, 2009, doi: 10.1109/TNSRE.2009.2018103.
- [2] H. Song, Y. Park, H. Kim, and H. Ko, "Fully integrated biopotential acquisition analog front-end IC," *Sensors (Switzerland)*, vol. 15, no. 10, pp. 25139–25156, 2015, doi: 10.3390/s151025139.
- [3] R. R. Harrison, "A Versatile Integrated Circuit for the Acquisition of Biopotentials," *Proc. IEEE 2007 Cust. Integr. Circuits Conf. CICC 2007*, no. Cicc, pp. 115–122, 2007, doi: 10.1109/CICC.2007.4405694.
- [4] R. R. Harrison *et al.*, "A wireless neural interface for chronic recording," *2008 IEEE-BIOCAS Biomed. Circuits Syst. Conf. BIOCAS 2008*, pp. 125–128, 2008, doi: 10.1109/BIOCAS.2008.4696890.
- [5] R. R. Harrison and C. Charles, "A low-power low-noise CMOS amplifier for neural recording applications," *IEEE J. Solid-State Circuits*, vol.

- 38, no. 6, pp. 958–965, 2003, doi: 10.1109/JSSC.2003.811979.
- [6] J. Holleman, “Design considerations for neural amplifiers,” *Proc. Annu. Int. Conf. IEEE Eng. Med. Biol. Soc. EMBS*, vol. 2016-October, pp. 6331–6334, 2016, doi: 10.1109/EMBC.2016.7592176.
- [7] S. Ha *et al.*, “Integrated circuits and electrode interfaces for noninvasive physiological monitoring,” *IEEE Trans. Biomed. Eng.*, vol. 61, no. 5, pp. 1522–1537, 2014, doi: 10.1109/TBME.2014.2308552.
- [8] L. Gupta and A. Kumar, “Comparison on Low-Noise Neural Signal Amplifiers and Design of Current Mirror OTA for EEG,” *Int. J. Pure Appl. Math.*, vol. 119, no. 12, pp. 14769–14784, 2018, [Online]. Available: <https://acadpubl.eu/hub/2018-119-12/articles/6/1382.pdf>.
- [9] M. Mollazadeh, S. Member, and K. Murari, “Micropower CMOS Integrated Low-Noise,” *IEEE Trans. Bio-medical Eng.*, vol. 3, no. 1, pp. 1–10, 2009.
- [10] X. Zou, W. S. Liew, L. Yao, and Y. Lian, “A 1V 22 $\mu$ W 32-channel implantable EEG recording IC,” *Dig. Tech. Pap. - IEEE Int. Solid-State Circuits Conf.*, vol. 53, pp. 126–127, 2010, doi: 10.1109/ISSCC.2010.5434024.
- [11] J. Wu, M. K. Law, P. I. Mak, and R. P. Martins, “A 1.83  $\mu$ W, 0.78  $\mu$ Vrms input referred noise neural recording front end,” *Proc. - IEEE Int. Symp. Circuits Syst.*, pp. 405–408, 2013, doi: 10.1109/ISCAS.2013.6571866.
- [12] W. M. Chen *et al.*, “A fully integrated 8-channel closed-loop neural-prosthetic cmos soc for real-time epileptic seizure control,” *IEEE J. Solid-State Circuits*, vol. 49, no. 1, pp. 232–247, 2014, doi: 10.1109/JSSC.2013.2284346.
- [13] L. H. C. Ferreira and S. R. Sonkusale, “A 60-dB Gain OTA operating at 0.25-V power supply in 130-nm digital CMOS process,” *Proc. - IEEE Int. Symp. Circuits Syst.*, vol. 0, pp. 1881–1884, 2014, doi: 10.1109/ISCAS.2014.6865526.
- [14] B. Razavi, *Design of Analog CMOS Integrated Circuits*, 2nd Editio. McGrawHill, 2005.
- [15] F. Shahrokhi, K. Abdelhalim, D. Serletis, P. L. Carlen, and R. Genov, “The 128-channel fully differential digital integrated neural recording and stimulation interface,” *IEEE Trans. Biomed. Circuits Syst.*, vol. 4, no. 3, pp. 149–161, 2010, doi: 10.1109/TBCAS.2010.2041350.
- [16] V. Majidzadeh, A. Schmid, and Y. Leblebici, “Energy Efficient Low-Noise Neural Recording,” vol. 5, no. 3, pp. 262–271, 2011.
- [17] W. Wattanapanitch, M. Fee, and R. Sarpeshkar, “An energy-efficient micropower neural recording amplifier,” *IEEE Trans. Biomed. Circuits Syst.*, vol. 1, no. 2, pp. 136–147, 2007, doi: 10.1109/TBCAS.2007.907868.
- [18] W. Zhao, H. Li, and Y. Zhang, “A low-noise integrated bioamplifier with active DC offset suppression,” *2009 IEEE Biomed. Circuits Syst. Conf. BioCAS 2009*, no. 60971084, pp. 5–8, 2009, doi: 10.1109/BIOCAS.2009.5372099.
- [19] M. Elzeftawi, S. Beach, L. Wang, and L. Theogarajan, “Capacitor-Integrated Electrodes for High Density Neural Implant Recording,” *Biomed. Circuits Syst. Conf. (BioCAS), 2012 IEEE*, pp. 236–239, 2012.
- [20] X. Zou *et al.*, “A 100-Channel 1-mW Implantable,” vol. 60, no. 10, pp. 2584–2596, 2013.
- [21] B. Gosselin, M. Sawan, and C. A. Chapman, “A low-power integrated bioamplifier with active low-frequency suppression,” *IEEE Trans. Biomed. Circuits Syst.*, vol. 1, no. 3, pp. 184–192, 2007, doi: 10.1109/TBCAS.2007.914490.
- [22] H. Sepehrian, S. A. Mirbozorgi, and B. Gosselin, “Multi-Channel Neural Signal Recording,” pp. 440–443, 2014.
- [23] K. A. Ng and Y. P. Xu, “A compact, low input capacitance neural recording amplifier,” *IEEE Trans. Biomed. Circuits Syst.*, vol. 7, no. 5, pp. 610–620, 2013, doi: 10.1109/TBCAS.2013.2280066.
- [24] P. L. Benko, M. Galeti, C. F. Pereira, J. C. Lucchi, and R. C. Giacomini, “Bio-amplifier based on MOS bipolar pseudo-resistors: A new approach using its non-linear characteristic,” *J. Integr. Circuits Syst.*, vol. 11, no. 2, pp. 132–139, 2016.
- [25] M. N. Sabry, H. Omran, and M. Dessouky, “Systematic design and optimization of operational transconductance amplifier using gm/ID design methodology,” *Microelectronics J.*, vol. 75, no. February, pp. 87–96, 2018, doi: 10.1016/j.mejo.2018.02.002.
- [26] M. Radfar, K. Shah, and J. Singh, “Recent subthreshold design techniques,” *Act. Passiv.*

- Electron. Components*, vol. 2012, 2012, doi: 10.1155/2012/926753.
- [27] M. Yin and M. Ghovanloo, "Using pulse width modulation for wireless transmission of neural signals in multichannel neural recording systems," *IEEE Trans. Neural Syst. Rehabil. Eng.*, vol. 17, no. 4, pp. 354–363, 2009, doi: 10.1109/TNSRE.2009.2023302.
- [28] V. Majidzadeh, A. Schmid, and Y. Leblebici, "A 16-channel 220  $\mu$ W neural recording IC with embedded delta compression," *2011 IEEE Biomed. Circuits Syst. Conf. BioCAS 2011*, pp. 9–12, 2011, doi: 10.1109/BioCAS.2011.6107714.
- [29] F. F. Zhang *et al.*, "Design of ultra-low power biopotential amplifiers for biosignal acquisition applications," *IEEE Trans. Biomed. Circuits Syst.*, vol. 1, no. 4, pp. 2–5, 2012, doi: 10.1109/TBCAS.2011.2177089.